Converter model

A solar generator is a form of a nonlinear process, which generates a maximal power at a particular operating voltage and current point. To control the delivered power to the Dc motor pump a DC-DC converter is inserted in series between the pump and the PV generator. Figure 5 shows the circuit diagram for the considered photovoltaic system.

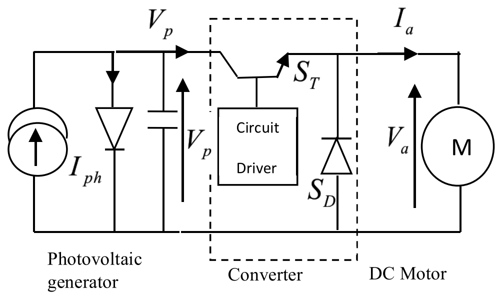

Figure 5. Equivalent circuit diagram of the photovoltaic system.

It can be noted that the convertor contains a circuit control driver related to power transistor (S_T) along with the free-wheel diode (S_D). The generated power is transmitted to the load using the switching transistor S_T that is turned on / off periodically using an external control circuit, identified as the *Pulse Width Modulation (PWM)*. Eq. (26) is describes the mean output voltage:

$$V_a = \rho V_p \tag{27}$$

wherein V_p and V_a represent the output and the converter-input voltage, respectively, and ρ refers to a switch cycle. Based on Eq. (26), it is obvious that the output voltage can be controlled by varying the ρ value of the chopper duty cycle. For varying ρ, the PWM design control of the process is applied (Packiam et al. 2015). Assuming the low power loss assumption, where the photovoltaic generated power is equivalent to the load consumed power, it comes:

$$V_p I_p = V_a I_a \tag{28}$$

$$\frac{V_p}{V_a} = \frac{I_a}{I_p} = \rho \tag{29}$$

DC motor pump model

The DC motor pump is a designed as a simple permanent magnet machine. In this study, it is assumed that the constant flow is present for all the operational points. In the machine model, R_a and R_L represent the resistance and the inductance. Furthermore, the equation below describes the transfer of energy between the electrical and the mechanical parts, which is shown as a relative proportion between the f.e.m. and the angular velocity:

$$E_a = k_b \Omega \tag{30}$$

The DC motor is attached to a centrifugal pump that for simplicity is described by the couple:

$$\Gamma = k_T \Omega \tag{31}$$

Therefore, the photovoltaic system model is written as

$$\begin{cases} \dot{i}_a = -\dfrac{R_a}{L_a} i_a - \dfrac{k_b}{L_a}\Omega + \dfrac{1}{L_p} v_p u \\ \dot{\Omega} = -\dfrac{kb}{J} i_a - \dfrac{k_T + F}{J}\Omega \\ \dot{v}_p = -\dfrac{u}{C} i_a - \dfrac{I_s}{C}\left[\exp\left(\dfrac{v_p}{V_T}\right) - 1\right] + \dfrac{I_{ph}}{C} \end{cases} \tag{32}$$

Writing system of Eq. (32) under the standard form yields

$$\begin{cases} \dot{x} = f(x) + g(x)u \\ y = h(x) \end{cases} \tag{33}$$

Wherein $x = \begin{bmatrix} i_a \\ \Omega \\ v_p \end{bmatrix}$ is the state vector comprising the motor current, motor speed and photovoltaic generator voltage.

Hence, one has

$$f(x) = \begin{bmatrix} -\dfrac{R_a}{L_a} i_a - \dfrac{k_b}{L_a}\Omega \\ -\dfrac{k_b}{J} i_a - \dfrac{k_T + F}{J}\Omega \\ -\dfrac{I_s}{c}\left[\exp\left(\dfrac{v_p}{V_T}\right) - 1\right] + \dfrac{I_{ph}}{C} \end{bmatrix}, \; g(x) = \begin{bmatrix} v_p \\ 0 \\ -i_a \end{bmatrix} \text{ and } y = h(x) = v_p$$

Estimating the relative degree r by deriving the equation output y until the control u appears:

$$\begin{aligned} \dot{y} = v &= \left[-u.i_a - I_s\left[\exp\left(\dfrac{v_p}{v_T}\right) - 1\right] + I_{ph}\right] \\ &= L_f h(x) + u.L_g h(x) \end{aligned} \tag{34}$$

The control input appears from the first derivation, which concludes the relative degree of the photovoltaic system is *r=1*.

Consequently, the control input can be written in the following form: $u = \alpha(x) + \beta(x)v$

Wherein $L_g h(x) = \dfrac{\partial h}{\partial x} g(x) = -\dfrac{i_a}{C}$

When the form of the dynamic feedback u polynomial equation is obtained, it is possible to establish the expression of the input-output linearizing control that yields:

$$\begin{aligned} u &= \frac{1}{L_g h(x)}\left(-L_f h(x) + v\right) \\ &= \frac{1}{i_a}\left[\left[-I_s \exp\left(\frac{v_p}{v_T}\right) - 1\right] + I_{ph}\right] - \frac{C}{i_a} v \end{aligned} \tag{35}$$

The main control achievement involves maintaining the optimal voltage for photovoltaic generator ($y(t) = v_p$).

Neglecting the reference variation, the objective can be fulfilled by selecting the control under the following form:

$$v = k\left(y_d - y\right) \quad (36)$$

wherein k refers to the control gain vector, which can be determined with a pole placement design.

Truncating the polynomial development to the third order for the photovoltaic model, and considering the nominal operating points $\left(X_n, U_n\right)$, leads to the polynomial model below:

$$\dot{x} = f_1 x + f_2 x^{[2]} + f_3 x^{[3]} \quad (37)$$

Furthermore, the polynomial form of the diffeomorphism truncated to the third order can be written as:

$$T\left(x\right) = T_1 x + T_2 x^{[2]} + T_3 x^{[3]} \quad (38)$$

Finally, the manipulated variable u is given by

$$u = \alpha_1 x + \alpha_2 x^{[2]} + \alpha_3 x^{[3]} + \mu_1 x + \mu_2 x^{[2]} + \mu_3 x^{[3]} \quad (39)$$

Simulation results

Table 2 presents the numerical values for the different parameters studied. The objective of this section is to evaluate the performance and efficiency of the studied control methods. The addressed control problem focuses on the tracking problem of a photovoltaic power system. In this study, all simulations are carried out using the MATLAB 2018 software.

Table 2. Numerical values of the model parameters.

Photovoltaic Generator	$I_{ph} = 4,4A$
	$I_S = 52,75.10^{-6} A$
	$V_T = 6.73V$
	$C = 4000.10^{-6} F$
DC Motor	$R_a = 1.072$
	$L_a = 0.05$
	$J = 476.10^{-6}$
	$F = 88.10^{-5}$
	$K_T = 14.10^{-4}$
	$K_b = 45.10^{-3}$

The first step of this study focused on the evaluation of the local performance of both controllers. The variation model represented by equation (37) is controlled to evaluate the local performance around an operating point. The state variables x_1, x_2 and x_3, are depicted in Figures 6, 7 and 8.

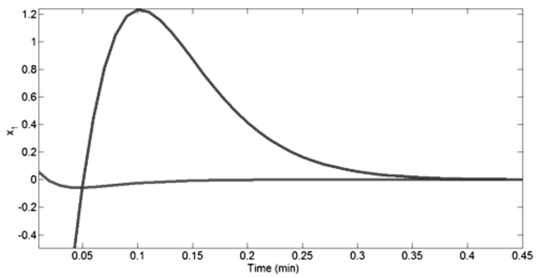

Figure 6. Dynamics of the variables x_1 (red): Neural case, (blue) Scheduling case).

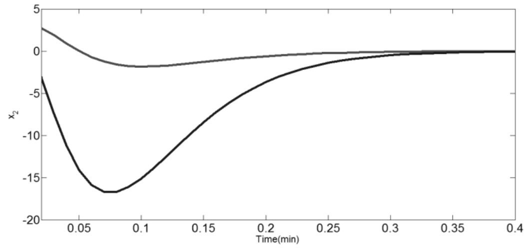

Figure 7. Dynamics of the variable x_2 ((red): Neural case, (blue) Scheduling case).

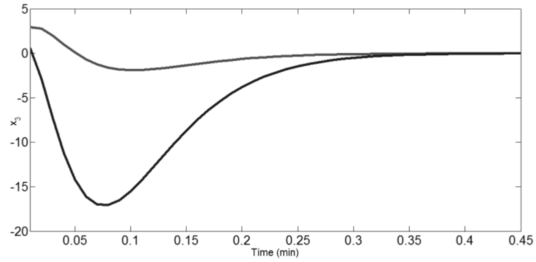

Figure 8. Dynamics of the variable x_3 ((red): Neural case, (blue) Scheduling case).

In these figures, the convergence of the state variables is ensured by both control techniques. The overall performance is quite satisfactory; with the state variables' dynamics being asymptotically stable with a swift transitory response and accurate steady state regime.

The figures have highlighted the acceptable dynamic behavior with a realistic the manipulated variable regulation. Likewise, it can be seen that the controlled variables for both cases are attracted towards the equilibrium and their dynamics does not indicate an inadmissible excess and overshooting. However, in terms of swiftness, a higher speed is noted for the scheduling gain-controlled variables. This result can be explained by the assumptions made while selecting the model truncating order and sampling time selection. Additionally, the feedback linearizing technique is very effective in compensating the plant nonlinearities as compared to the polynomial neural network.

Figure 9 represents the control inputs. The latter manage to stabilize the system dynamics within a limited time period with a reduced control effort. In particular, the neural network stabilizes the system dynamics within 0.2 minutes; however, the scheduling control stabilizes the state variables within 0.3 minutes. Table 3 summarizes the key parameters that were obtained by qualitatively analyzing the response times for the transient and steady-state responses. regime. The scheduling approach offers a settling time of 3 s, while the neuronal approach displayed a settling time of 0.12 s.

Likewise, the gain scheduling technique helped in achieving a rise time in 0.2 s however the rise time is 0.09 s for the neural control approach.

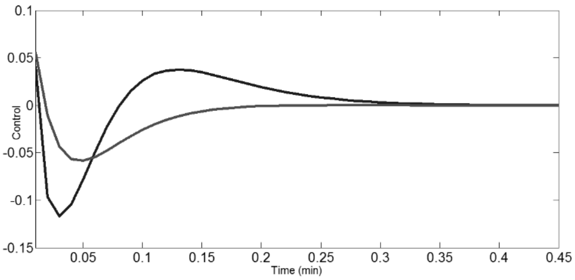

Figure 9. Control input dynamics *u* ((red): Scheduling case, (blue) Neural case).

Table 3. Numerical results of the qualitative comparative study.

	Gain Scheduling approach	Neuronal approach
Settling Time	0.3s	0.12s
Overshooting	No	No
Rise Time	0.2s	0.09s

As a first outcome the neural control approach displayed better local elementary results as compared to the gain scheduling approach. Furthermore, satisfactory dynamical results were noted with a smoother response time for the model state variables.

In the next stage of this analysis study, the learning process based on the multilayer neural networks and using the gradient approach to assess the weights by decreasing the costs will be addressed.

Here, the learning process is known as the learning with the error retro-progression. For carrying out this process and conducting the online learning, the following steps are used:

- The structure of the neural networks is shown in Figure 1

The estimation of the error is performed using an approach that decreases the output squared learning error. As a matter of fact, the error can be defined as: $E = \left\{ \left\| x - \hat{x} \right\| \right\}$

Figure 10 presents the simulation results. It can be seen that the quadratic error for all the state variables tends towards 0; hence, the system stability can be guaranteed by applying the neuronal method.

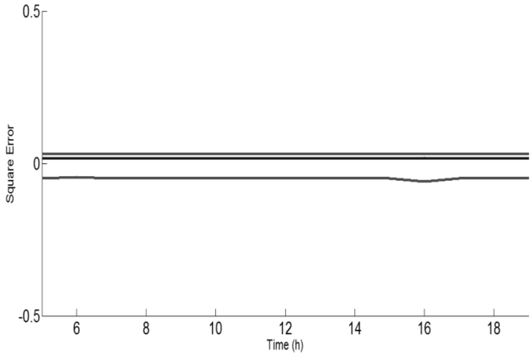

Figure 10. Square error for the different states.

The final stage of this study is reserved for the key studied problem in this paper, which is the trajectory tracking control problem. The desired output trajectory is shown in Figure 11. This trajectory defines a standard physical behavior in terms of the system characteristics and features.

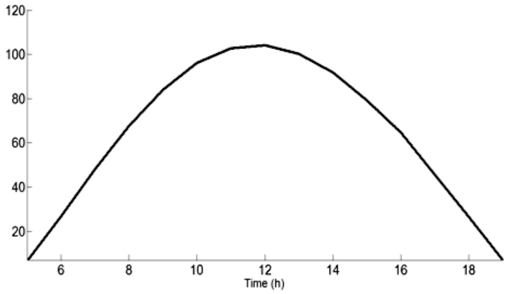

Figure 11. Desired output trajectory.

After carrying out the simulation study, the results are presented in Figure 12. A perfect agreement can be noted for all different trajectories.

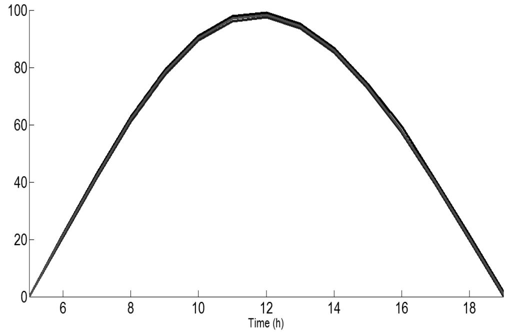

Figure 12. Output tracking trajectory ((black): Desired output trajectory, (red): Neural output trajectory, (blue): Gain scheduling output trajectory).

Correspondingly, the transient responses show that the real outputs for both techniques converge towards the desired output trajectory while the behaviour of the controlled variables does not show an inadmissible dynamic.

To emphasize the performances of the gain scheduling and the neuronal approaches, it is interesting to note that the tracking error is less than 2% for the scheduled gain approach. However, for the neural control, an error of < 1.6% was measured. This result is depicted in Figure 13.

The controllers were evaluated in real time. Therefore, the total time for carrying out these tasks did not greatly affect the system variable dynamics or the desired output trajectory.

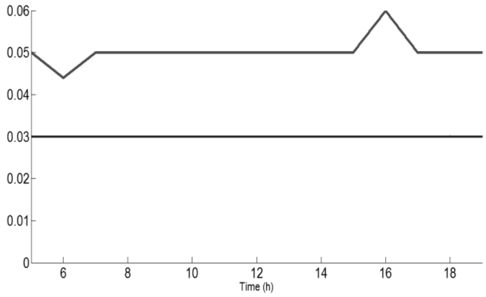

Figure 13. The tracking error ((blue): neuronal approach, (red): gain scheduling approach).

Figure 14, describes the control input dynamics for the studied approaches. The control signals dynamics are physically satisfactory. The figure showed that there was no undesired overshoot or an undesirable saturation for both approaches. Similarly, a limited control effort for the system state variable stabilization can be noted.

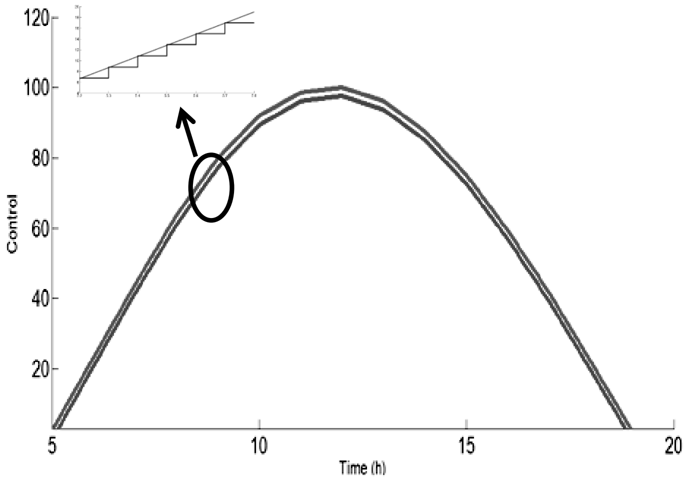

Figure 14. Control inputs dynamics ((blue): Neuronal case, (red): Scheduling case).

It is perceived that the tracking error was quite weak; however, a tracking error is still seen in this study. Moreover, this tracking error did not show a significant physical effect. Decreasing its value can be assured by increasing the number of the operating points on the desired output trajectory. These overall results helped in concluding that the studied approaches are comparable in performance level and practical efficiency.

Likewise, it can be also observed that the neural approach showed better results than the gain scheduling method. This is due to an enhanced methodology in selecting of controller gains by combining the subsequent operating points.

CONCLUSIONS

In this paper, a critical comparative analysis of an analytical approach with an advanced computing control technique is performed. The performance analysis is conducted for a PV solar power plant. Recent scheduled gain control theory is efficiently exploited as an analytical control strategy. Such theory helped assess and compute the operating state feedback gains of a stabilizing controller, which contributes to bringing the power electrical system to its nominal operating conditions following desired output trajectory constraints. The gain scheduling approach relied on the formalism of feedback linearization, gain scheduling methodology, variation based-model concept, and a non-Lyapunov stability method. It can be assumed that the gain scheduling technique can fulfil the objective of a trajectory tracking with high performance standard. Furthermore, it could be seen that it was conceptually simple; therefore, it could be easily applied.

The simulation results reflect that the designed controller offers enhanced dynamic performances than various available methods in the literature. This is in terms of attenuated oscillations, minimum settling time numerical values, peak undershoot, peak overshoot, various performance indices and minimum numerical values for damping ratio. The maximization of the attraction domain around equilibrium points substantiates the output dynamic stability behavior of the systems compared to several prevalent control techniques. Nevertheless, the gain scheduling approach, due to the drawback of the linearization approach, ensures the design strategy efficiency only in regions, which are relatively close to the operating points.

On the other hand, the neuronal control approach displayed satisfactory results in recovering and compensating the hard nonlinearities of the studied plant. However, it has restrictions related to the training phase and its data structure.

Indeed, several parameters must be taken into account as the prediction of the operating points, the dynamical stability behavior and the optimal control gains.

- Lastly, the following practical points can be addressed as further extensions for developing this work: it is promising to estimate uncertain states and different model parameters for implementing the control laws and ensuring the fault detection with disturbances rejection.

REFERENCES

Andoulsi, R., Mami, A., Dauphin-Tanguy, G. & Annabi, M. 1999. Modelling and simulation by bond graph technique of a DC motor fed from a photovoltaic source via MPPT boost converter. Proceeding of CSSC, **99**: 4181-4187.

Andoulssi, R., Draou, A., Jerbi, H. 2013. Nonlinear control of a photovoltaic water pumping system. Energy Procedia. **42**: 328-336.

Campos, S. & Lewis, F.L., 1999. Dead zone compensation in discrete time using adaptive fuzzy logic. IEEE Transactions on Fuzzy Systems. **7**(6): 697-707.

Chaouech, H., Charfeddine, S., Ouni, K., Jerbi, H. & Nabli, L. Intelligent supervision approach based on multilayer neural PCA and nonlinear gain scheduling. NCAA: Neural Computing and Applications. **31**(3):1-11.

Charfeddine, S. & Jerbi, H. 2012. A Survey on nonlinear gain scheduling design control for continuous and discrete time. International Journal Modelling, Identification and Control. **19**(3): 203-216.

Charfeddine, S. & Jerbi, H. 2012. Trajectory tracking and disturbance rejection for nonlinear periodic process: A gain scheduling design. IREMOS: International Review on Modelling and Simulations. **5**(2): 1075-1083.

Charfeddine, S., Jerbi, H. & Sbita, L. 2013. Non-Linear Discrete –Time Gain Scheduling Control for Affine Non-Linear Polynomial Systems. IREMOS: International Review on Modelling and Simulations. **6**(3): 1031-1041.

Chemachema, M. & Belarbi, K. 2010. State feedback linearization-based neural network adaptive control for a class of uncertain SISO nonlinear systems. International Journal Modelling, Identification and control. **11**(1-2): 44-51.

Dahleh, M.A., McConley, M.W., Appleby, B.D. & Feron, E. 2000. A computationally efficient lypunov-based scheduling procedure for control of nonlinear systems with stability guarantees. IEEE Transactions Automatic Control. **45**(1): 33-49.

Deutscher, J. 2005. Input-output linearization of nonlinear systems using multivariable Legendre polynomial. Automatica. **41**(2): 299-304.

Feng, G. 2006. A survey on analysis and design of model-based fuzzy control systems. IEEE Transactions on Fuzzy Systems. **14**(5): 676-697.

Genesio, R., Tartaglia, M. & Vicino, A. 1985. On the estimation of asymptotic stability regions: State of the art new proposals. IEEE Transactions on the Automatic Control. **30**(8): 747-755.

Hamdy, M. 2013. State observer based dynamic fuzzy logic system for a class of SISO nonlinear systems. International Journal of Automation and Computing. **10**(2): 118-124.

Hespanha, J.P., Naghsh, Tabrizi, P. & Xu, Y. 2007. A survey of recent results in networked control systems. Proceedings of the IEEE. **95**(1): 138-162.

Isodiri, A. 1998. Nonlinear Control Systems. 2nd ed. New York: Springer.

Jebri, W., Jerbi, H. & Abdelkrim, M.N. 2011. Nonlinear state feedback design for continuous polynomial systems. International Journal of Control, Automation and Systems. **9**(2): 566-573.

Jerbi, H. 2017. Estimations of the domains of attraction for classes of nonlinear continuous polynomial systems. Arabian Journal for Science and Engineering. **42**(7): 2829-2837.

Kanellakopoulos, I., Kokotovic, P.V. & Marino, R. 1991. An extended direct scheme for robust adaptive nonlinear control. Automatica, **27**(2): 247-255.

Landau, I. & Silveira, H. 1979. A stability theorem with applications to adaptive control. IEEE Transactions on Automatic Control. **24**(2): 305-312.

Liu, Y. & Tong, S. 2015. Adaptive fuzzy control for a class of unknown nonlinear dynamical systems. Fuzzy Sets and Systems. **263**: 49-70.

Miamouni, M.F., Mansori, M.N., Benghanem, B. & Annabi, M. 2004. Vectoriel command of an asynchronous motor fed by photovoltaic generator. Renewable Energy. **29**: 433-442.

Narendra, K.S. & Parthasarathy, K. 1990. Identification and control of dynamical systems using neural networks, IEEE Transactions Neural Networks. **1**(1): 4-27.

Narendra, K.S. & Parthasarathy, K. 1991. Gradient methods for the optimization of dynamical systems containing neural networks, IEEE Transactions Neural Networks. **2**(2): 252-262.

Palm, R., Driankov, D. & Rehfuess, U. 1996. A Takagi-Sugeno fuzzy gain-scheduler. Proceedings of the 5th IEEE International Conference, Fuzzy Systems. **2**: 1053-1059.

Palm, R., Stutz, C. & Runkler 2000. A control sequence generator for fuzzy gain schedulers, Proceedings of the 39th IEEE Conference Decision and Control. **1**: 370-375.

Packiam, P., Jain, N.K. & Singh, I.P. 2015. Steady and transient characteristics of a single stage PV water pumping system. Energy Systems. **6**: 173-199.

Sadegh, N. 1993. A perceptron network for functional identification and control of nonlinear systems, IEEE Transactions Neural Network, **4**: 982-988.

Sadati, H., Sabzehparvar, M., Menhaj, M.B. & Bahrami, M. 2007. Backstepping controller design using neural networks for a fighter aircraft. European Journal of Control. **13**(5): 516-526.

Sardellitti, I., Medrano-Cerda, G.A., Tsagarakis, N., Jafari, A. & Caldwell, D.G. 2013. Gain-scheduling control for a class of variable stiffness actuators based on lever mechanisms. IEEE Transactions on Robotics. **29**(3): 791-798.

Sato, M. & Peaucelle, D. 2013. Gain-scheduled output-feedback controllers using inexact scheduling parameters for continuous-time LPV systems. Automatica. **49**(4): 1019-1025.

Souza, C.E. & Osowsky, J. 2013. Gain-scheduled control of two-dimensional discrete-time linear parameter-varying systems in the Roesser model. Automatica. **49**(1): 101-110.

Werbos, P.J. 1989. Maximizing long-term gas industry profits in two minutes in lotus using neural network methods. IEEE Transactions Systems Man. Cybernetics. **19**(2): 315-333.

Yu, C. & Verhaegen, M. 2018. Data-driven fault estimation of non-minimum phase LTI systems. Automatica. **92**: 181-187.